ACS OMEGA

Open Access

http://pubs.acs.org/journal/acsodf

Article

Enhancement of Thermal and Gas Barrier Properties of Graphene-Based Nanocomposite Films

Jaweria Ashfaq, Iftikhar Ahmed Channa,* Abdul Ghaffar Memon, Irfan Ali Chandio, Ali Dad Chandio, Muhammad Ali Shar, Mohamad S. Alsalhi, and Sandhanasamy Devanesan

Cite This: *ACS Omega* 2023, 8, 41054−41063

Read Online

ACCESS | Metrics & More | Article Recommendations

ABSTRACT: Poly(vinyl alcohol) (PVA), a naturally occurring and rapidly decomposing polymer, has gained significant attention in recent studies for its potential use in pollution preventive materials. Its cost-effectiveness and ease of availability as well as simple processing make it a suitable material for various applications. However, the only concern about PVA's applicability to various applications is its hydrophilic nature. To address this limitation, PVA-based nanocomposites can be created by incorporating inorganic fillers such as graphene (G). Graphene is a two-dimensional carbon crystal with a single atom-layer structure and has become a popular choice as a nanomaterial due to its outstanding properties. In this study, we present a simple and environmentally friendly solution processing technique to fabricate PVA and graphene-based nanocomposite films. The resulting composite films showed noticeable improvement in barrier properties against moisture, oxygen, heat, and mechanical failures. The improvement of the characteristic properties is attributed to the uniform dispersion of graphene in the PVA matrix as shown in the SEM image. The addition of graphene leads to a decrease in water vapor transmission rate (WVTR) by 79% and around 90% for the oxygen transmission rate (OTR) as compared to pristine PVA films. Notably, incorporating just 0.5 vol % of graphene results in an OTR value of as low as 0.7 cm m^{-2} day^{-1} bar^{-1}, making it highly suitable packaging applications. The films also exhibit remarkable flexibility and retained almost the same WVTR values even after going through tough bending cycles of more than 2000 at a bending radius of 2.5 cm. Overall, PVA/G nanocomposite films offer promising potential for PVA/G composite films for various attractive pollution prevention (such as corrosion resistant coatings) and packaging applications.

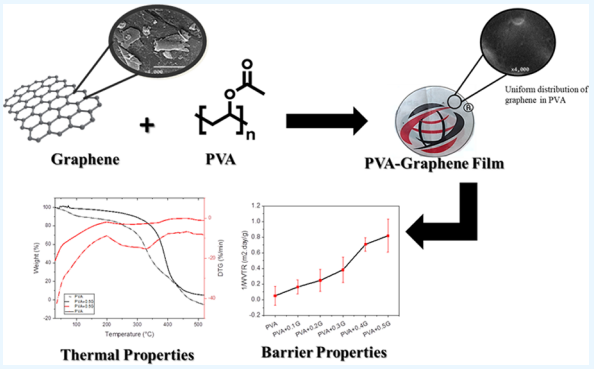

1. INTRODUCTION

Polymers offer a variety of excellent environmental and physical features such as density, linearity, humidity, molecular weight, crystallinity, and more, making them highly competitive in the food packaging industry.[1] The industry frequently requires materials with specific degrees of polymerization, chemical inertness, water and oxygen permeability, density, thermal properties, mechanical properties, and morphological properties[2] all of which polymers can provide. Unfortunately, nonbiodegradable polymers are commonly used in food packaging, contributing to environmental problems.[3,4] It is crucial to use polymers that decompose easily and quickly to reduce environmental pollution. Biopolymers are the ideal solution because they are biodegradable, environmentally friendly, and renewable[5−8] The remarkable properties of biopolymers make them suitable for a wide range of applications. Biopolymers can be divided into two types: natural or synthetic. Natural biopolymers include proteins, polysaccharides such as cellulose and starch, and others, while synthetic biopolymers include polylactic acid (PLA),[9] poly(vinyl alcohol) (PVA),[10] polycaprolactone (PCL),[11] polyhydroxy butyrate (PHB),[12] and polyglycolic acid (PGA).[13] These materials have applications in the medical, textile, and packaging industries. The only limitation to using biopolymers may be their unfavorable mechanical and barrier properties due to their hydrophilic nature. However, incorporating nanoparticles into these polymers and using them as polymer nanocomposites[5,14] can solve this problem.

Poly(vinyl alcohol), also known as PVA, is a synthetic and relatively inert polymer that is water-soluble. It is a biocompatible and biodegradable polymer with many

Received: April 27, 2023
Revised: October 9, 2023
Accepted: October 12, 2023
Published: October 25, 2023

applications in different industries, such as packaging and adhesives.[15] PVA is a semicrystalline and nontoxic material with excellent thermal stability, high transparency, good mechanical properties, flexibility, and high gas barrier properties. Poly(vinyl alcohol) (PVA)'s solubility in water and its tendency to absorb water can pose challenges in applications requiring gas barrier qualities. To address this, researchers use cross-linking PVA molecules, adding hydrophobic polymers, and controlling hydrolysis during production. They also insert hydrophobic agents or surface modifiers to prevent water penetration while maintaining gas barrier properties. Production process variables like temperature, pressure, and humidity also improve PVA's water solubility and gas barrier performance. Barrier coatings or laminates protect PVA from direct moisture exposure, ensuring that its gas barrier properties remain intact. The final PVA product is tested and controlled to meet the required standards for reduced water absorption and gas barrier qualities. These scientific techniques effectively address the challenges posed by PVA's water solubility and water absorption while maintaining its essential gas barrier properties in various applications. Its excellent processability and film-forming ability make PVA films easy to fabricate by casting or blow extrusion.[16−18] To enhance the thermal and barrier properties of PVA, nanoparticles are often employed. Nanotechnology, which involves engineering materials with at least one dimension in the nano range (10−100 nm),[19] offers a way to gain new characteristics attributed to nanometer dimensions. One of the best and fastest routes to apply nanotechnology is by creating nanocomposites. Polymer nanocomposites have been used as barrier films to protect OLEDs, photovoltaics, food, medicines, drinks, and in many other applications because of their low cost, environment-friendly processing and lightweight.[20] Barrier films are designed to hinder gas and moisture permeation through them, which can be detrimental to packaged food quality.[21] Different methods can be used to decrease the permeability of polymers, but the best alternative material is adding nanosized inorganic fillers, which possess a great boundary volume and fine grain size, such as clay,[22] silica particles,[23] ZnO,[24] carbon nanotubes,[25] graphene,[26] graphene oxide,[27] etc.[28] A polymer nanocomposite coating consists of polymer matrices and nanofillers (usually inorganic nanoparticle fillers), such as metal oxides, SiO_2, ZnO, Al_3O_2, TiO_2, clay, graphene, graphene derivatives, carbon nanotubes, etc. Graphene is an extremely unique substance with a honeycomb lattice and a single sheet of sp^2 carbon atoms. It is the stiffest, strongest, but thinnest material known.[29] It has been used in numerous sectors such as electronic, optical, light processing, mechanical, energy-related, thermal, and distinct biological, making it a low-cost material that can be utilized to improve the performance of a polymer.[26] Graphene enhances the mechanical properties of composite materials by increasing their aspect ratios and covalent bonding. This increases tensile strength and Young's modulus, making it a more durable material. Graphene also distributes loads and transfers stress, increasing its mechanical resilience. However, variable water contents can affect mechanical strength in gas barrier applications as some polymers can be plasticized and softened by water, lowering the overall strength. To maintain mechanical robustness and gas barrier performance under various aqueous conditions, careful selection of polymer matrix and graphene concentrations is crucial. Singh et al.[30] studied graphene-based materials for gas and chemical sensors in wearable electronics, focusing on sensitivity and selectivity in hazardous gases, heavy metals, and environmental contaminants. They investigated potential applications in wearable electronic devices and the IoT, addressing challenges like flexibility, stability, and wireless integration. Other researchers like Tambe et al.[31] synthesized a PVA/graphene solution to spin coat graphene over a steel substrate. As the concentration of graphene in the PVA matrix nanocomposite coating on the steel substrate increased, the coefficient of friction also increased. A nanocomposite with improved mechanical strength, thermal stability, and electrical conductivity compared with pure PVA is produced by incorporating graphene into the PVA matrix. High aspect-ratio graphene and powerful covalent bonds enhance mechanical qualities like tensile strength and Young's modulus, making these nanocomposites appealing for structural applications. Additionally, because of the high thermal conductivity of graphene, the PVA matrix has better thermal stability, increasing its usefulness under hot conditions. By addition of graphene, it is possible to dramatically increase the electrical conductivity of PVA, which opens up opportunities for use in flexible electronics, sensors, and conductive coatings. Graphene can be added to PVA to enhance its gas barrier qualities, which makes these nanocomposites potentially useful as barrier coatings and packaging materials.[31] Krishnan et al.[32] studied the graphene-based nanocomposite. In this research, biosensors are crucial in medical sciences for precise physiological evaluation. Graphene-based nanocomposites offer efficient, cost-effective solutions for biosensor development. These platforms detect various biomolecules with low detection limits, enabling biofunctionalization, enzyme immobilization, and various reactions on nanocomposite surfaces.

To produce polymer matrix nanocomposites, researchers have explored several methods, including melt mixing, in situ polymerization, and mixing filler ingredients while electrospinning. However, these techniques can be expensive.[33,34] The simplest and most effective method for fabricating polymer-based nanocomposites is solution mixing. This involves mixing colloidal suspensions of nanoparticles with polymer matrix solutions through simple stirring or shear mixing. The nanocomposite can then be recovered using solvent evaporation, distillation, or no solvent coagulation. Blade casting is another environmentally friendly method for producing nanocomposites, where a hot melt or solution is cast on substrates such as polyester or PET depending on the polymer and composite nature. The thickness of the film and the content of the casting resin can be controlled by a doctor's blade or film applicator. This method allows for the easy dispersion of nanoparticles without agglomeration. Vollenberg and Heikens[35] produced nanocomposite samples by thoroughly mixing filler particles with a polymer matrix. They used filler materials such as alumina beads with 35 and 400 nm dimensions and mixed them with polystyrene (PS), styrene-acrylonitrile copolymer (SAN), polycarbonate (PC), and polypropylene (PP). The average volume fraction of filler particles was maintained at 25%.

The main objective of this study is to create coatable thin films of PVA-based nanocomposites. Produced thin films will have PVA as a matrix and graphene nanosheets as nanofillers. The films will be produced by the cost-effective method, i.e., blade coating, as to mimic the high throughput roll-to-roll coating method. The cost-effective thin films will have improved barrier characteristics against heat and environ-

https://doi.org/10.1021/acsomega.3c02885
ACS Omega 2023, 8, 41054−41063

mental attacks such as the diffusion of oxygen and moisture while maintaining the transparency. This coatable PVA-based solution can be applied to a variety of applications wherein thermal stability and barrier against diffusion of gases is prime requirement such as packaging of food or electronics and corrosion resistant applications for textile and polymeric items.

2. MATERIAL AND METHODS

2.1. Materials. The PVA used in this study was purchased from Aldrich Chemistry (Darmstadt, Germany) and had an average M_w of 85,000−124,000 and an 87−89% hydrolyzed content. Graphene nanoparticles with an α value of 200 were supplied by Aldrich Chemistry (Darmstadt, Germany).

2.2. Sample Preparation. The following method was used to prepare PVA/graphene nanocomposite films. First, 1 g of PVA powder was added slowly to 100 mL of distilled water at 90 °C and stirred for 1 h using a magnetic stirrer at 700 rpm. Graphene was dispersed in distilled water using ultra sonication. Next, the desired amount of graphene dispersion was gradually added using a glass dropper into the PVA solution and stirred for 1 h. To investigate the effect of the filler content on the characteristics of the nanocomposite, the weight percentage of graphene was varied from 0.1 to 0.5 vol %. Lower filler content was chosen to prevent agglomeration, which would weaken the thermal properties of the nanocomposite. High filler content would likely cause the filler to clump together in the nanocomposite. The PVA/graphene solution was then ultra sonicated again for 20 min to prevent agglomeration.

The next step involved blade casting of the solution with the thickness of the applicator set at 50 μm. The resulting thin films were left to dry at room temperature for 24 h. The films were kept in a vacuum desiccator until further characterization was performed.

2.3. Characterization. *2.3.1. UV−Vis Spectrophotometry.* The UV/vis absorption spectra of the single photoactive layers (P3HT) were measured using a Shimadzu UV-1800 spectrophotometer. To ensure that the sample is hit at the same spot during the degradation test at various time intervals, a customized sample holder was utilized.

2.3.2. Fourier Transform Infrared (FTIR) Spectrophotometry. The FTIR spectra were recorded in ATR mode using a Bruker ALPHA-P FTIR spectrophotometer (operated with OPUS 7.2 software) in 64 scan summations at a resolution of 4 cm^{-1}.

2.3.3. Scanning Electron Microscopy. The JSM-7610F type of JEOL scanning electron microscope (SEM) was used for the morphological investigation. A secondary electron image detector was used to produce high-resolution topographical imaging. The 20 kV accelerating voltage and a low probe current mode set to 65 nA were found to be the ideal operational conditions. Notably, the polisher played a critical role in the sample preparation procedure.

2.3.4. Tensile Strength. Tensile strength (TS) and elongation at break (EAB) of each film were evaluated using Z005 Zwick/Roell universal testing equipment from Germany. The samples were prepared in accordance with ASTM D 882-10 guidelines, using a crosshead speed of 5 mm/min and a starting grab separation of 50 mm. The films were divided into strips that were 130 mm long and 30 mm wide. To evaluate the samples' mechanical qualities, a 5N load cell was employed.

2.3.5. Water Vapor Transmission Rate (WVTR). A Thwing−Albert Instrument Company (West Berlin, NJ, USA) aluminum cup with a diameter of 6.35 cm, complying with the ASTM E-96 standard, was used. The experiment was conducted according to the methodology outlined by Channa et al.[36]

2.3.6. Bending. A cyclic bend tester was used where one end was stationary and the other end moved forward and backward to create a radius with a predetermined value. The film's resistance to bending was determined after each set of bending cycles, and the sample size for this test was 3 × 10 cm^2. A sample measuring 3 × 3 cm^2 was taken from the center of the bent sample for the permeation test.

2.3.7. Oxygen Transmission Rate Measurement of Films. The oxygen penetration rate was measured using a permeation chamber with an optical oxygen measuring spot, Pst9, made by PreSens Precision Sensing GmbH, Regensburg, Germany. The detection limit for oxygen permeation was 0.1 cm^3 m^2 day^{-1} bar^{-1}. The oxygen transmission rate (OTR) and permeability were calculated after the samples were positioned between the two chambers of the device and after 15 min of nitrogen gas flow in each permeation cell. Oxygen was then pumped for 30 s in the bottom chamber, and the increase in oxygen fraction in the top chamber was continually examined for a few days.

2.3.8. Thermogravimetric Analysis (TGA). The thermal stability of the films was investigated using a thermogravimetric analyzer (SDT Q-600 TA Instruments, Artisan Technology Group, Champaign, IL, USA). The initial sample weight for each operation was set at 5−8 mg, and the sample was heated from 24 to 550 °C at a rate of 10 °C/min in a nitrogen environment using a low flow rate of 200 mL/min.

3. RESULT AND DISCUSSION

3.1. Transparency. The main challenge for food packaging is to achieve a transparent barrier coatings. Figure 1 illustrates

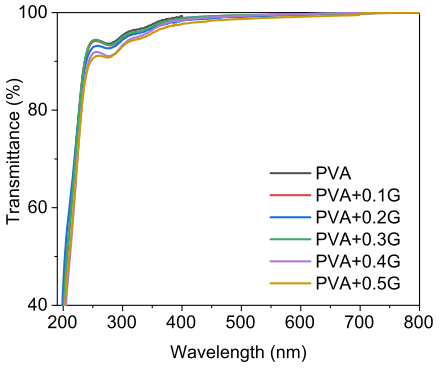

Figure 1. UV−vis spectra of PVA and PVA/graphene nanocomposite films between the wavelength of 200−800 nm.

the UV−vis spectra of PVA and its nanocomposites with graphene. The pure PVA film exhibited high transparency across the visible light range (380−800 nm) with a total transmittance of 98% at 550 nm, making it suitable for optical applications such as polarizers or long-pass filters.[31,37] However, for the nanocomposites, the total transmittance remained almost unchanged, even after the addition of graphene content. A negligible decrease in transmittance was observed, which could be attributed to either the scattering of a small portion of light due to graphene particles or reflectance. Therefore, the maintenance of the transparency of the barrier nanocomposite is solely dependent on the graphene content within the matrix.[38] Figure 2 represents the optical trans-

https://doi.org/10.1021/acsomega.3c02885
ACS Omega 2023, 8, 41054−41063

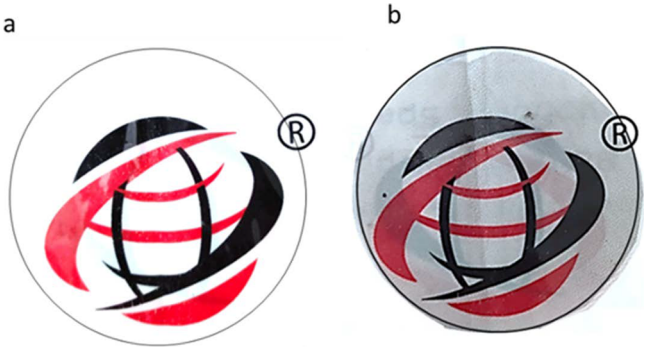

Figure 2. Optical transparency of (a) pure PVA film and (b) PVA with 0.5 vol % graphene film with logo on the back side. A black circle has been drawn around the sample.

parency of PVA and the PVA/G nanocomposite, indicating no difference in transparency. Similarly, Figure 3 shows transmittance measurements at 550 nm, indicating a decrease in total transmittance with increasing graphene content.[39]

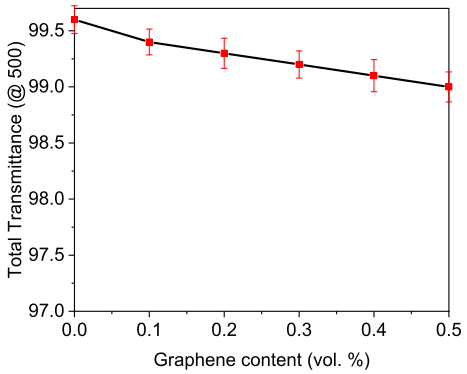

Figure 3. Total transmittance of barrier films with 0−0.5 vol % graphene@550 nm extracted from UV−vis spectra.

3.2. Compound Analysis via FTIR. The FTIR spectra of graphene, pure PVA film, and PVA/graphene nanocomposite films are presented in Figure 4. Graphene shows two distinct peaks at 1350 and 1620 cm^{-1}, which are also observed in the polymer and polymer nanocomposite films. The bands at 1088 cm^{-1} are attributed to the vibrational movement of functional

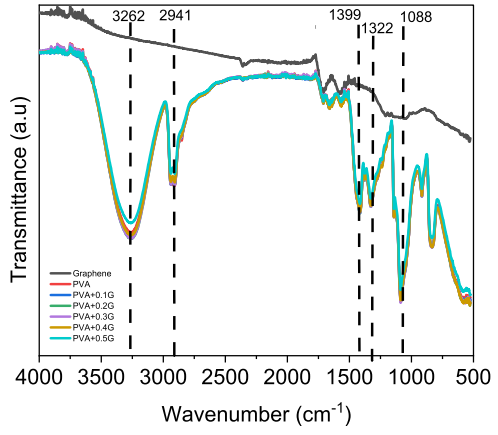

Figure 4. FTIR spectrum of graphene, PVA, and PVA/G nanocomposite barrier films with different graphene vol %.

groups such as C−O (bending) present in PVA. The peaks at 1322 and 1399 cm^{-1} are due to C═O bending. The two weak bands at 2907 and 2941 cm^{-1} can be attributed to C−H stretching and the existence of acetate groups in the PVA matrix.[40] The peaks at 3262 cm^{-1} are assigned to normal polymeric O−H stretching, which is a result of intermolecular as well as intramolecular hydrogen bonds present in the PVA matrix.[41] The addition of graphene did not lead to any change in the molecular interactions. Graphene and PVA (poly(vinyl alcohol)) with graphene may have similar FTIR spectra because the FTIR technique primarily measures the vibrational modes of chemical bonds in a material, and the presence of graphene in the PVA matrix may not significantly alter the fundamental chemical structure of PVA. Graphene is made up of carbon atoms organized in a 2D honeycomb lattice and lacks major distinctive absorption bands in the FTIR region. As a result, its presence in a composite material such as PVA with graphene may not result in distinguishable peaks in the FTIR spectrum. PVA, on the other hand, is a polymer composed of repeated $-CH_2-CH(OH)-$ units, and its FTIR spectrum often exhibits peaks associated with these functional groups. The chemical structure of PVA is not greatly altered when graphene is integrated into the PVA matrix, so the FTIR spectrum of the composite material may closely mirror that of pure PVA.[42]

3.3. Microstructure. The SEM image of the complicated structure of the graphene nanoflakes is shown in Figure 5a. The graphene structures presented by Mutyala and Mathiyarasu[43] are also comparable. Due to their distinct presence within the substrate, these tiny graphene flakes appear as discrete entities. The SEM image provides a high-resolution perspective that enables the in-depth analysis of these graphene nanoflakes because it was created at an accelerating voltage of 20 kV, was magnified by a factor of 4000×, and covered a 5 μm area. Figure 5b,c, which exhibits PVA composite material with a 0.5% graphene content, then reveals a unique characteristic. At this particular condition, the SEM pictures clearly show a remarkable degree of homogeneous incorporation of graphene throughout the whole PVA matrix. Notably, there are no discernible fluctuations or clusters of graphene, demonstrating that the material has achieved a remarkably uniform dispersion of graphene within the polymer. This consistency is particularly important because it ensures that graphene's excellent features, such as great electrical conductivity and increased mechanical strength, are consistently integrated throughout the entire composite material.[44]

3.4. Bending. Bendability and flexibility at a smaller radius are two of the most desirable characteristics of films.[18] To demonstrate the produced films' flexibility, a bending test was conducted and the outcomes are presented in terms of normalized WVTR (as shown in Figure 6). The films were bent with a radius of 6.35 cm, and identical films were then analyzed for WVTR. If the bent film maintains its initial WVTR even after multiple bending cycles, it would indicate that the films are flexible and bending does not impair their functionality (WVTR). Therefore, 20,000 bending cycles were applied to all created films, and they were frequently checked for WVTR. The results of the first and periodic WVTR studies were the same, indicating that perfect PVA films displayed exceptional bendability. This suggests that PVA films were unaffected even after 20,000 bending cycles. Additionally, the films showed no obvious signs of degradation after being bent. However, PVA films containing graphene also showed a

https://doi.org/10.1021/acsomega.3c02885
ACS Omega 2023, 8, 41054−41063

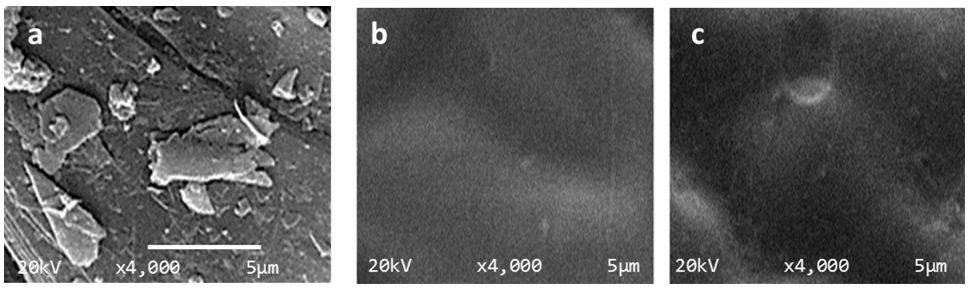

Figure 5. SEM images of graphene and their composite. (a) Nano flakes of graphene, (b) PVA with 0.1% graphene, and (c) PVA with 0.5% graphene.

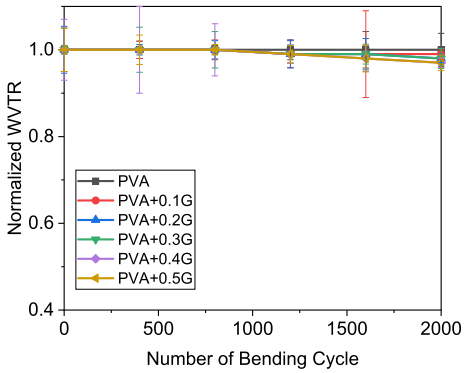

Figure 6. Normalized WVTR values of different concentrations of graphene film with 0−0.5 vol % films plotted against the number of bending cycles at a bending radius of 6 cm. The black curve represents the pristine PVA film, the red curve represents the PVA + 0.1G, the blue curve represents the PVA + 0.2G, the green curve represents the PVA + 0.3G, the purple curve represents the PVA + 0.4G, and the yellow curve represents the PVA + 0.5G vs the number of bending cycles. All the rested films had a thickness of 100 μm.

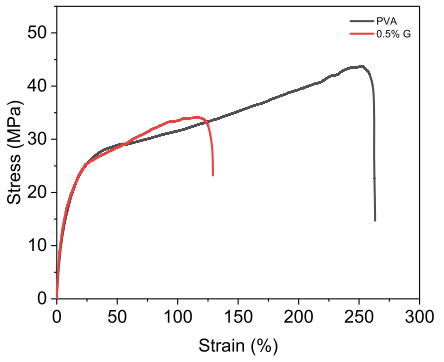

Figure 7. Stress−strain relationships of PVA and PVA/GO nanocomposite films.

negligible change in the composite coatings. PVA films containing 0, 0.1, 0.2, 0.3, 0.4, and 0.5 vol % graphene, respectively, showed losses of 0.1−0.3%. This could be explained by the strong link or wetting between PVA and graphene 2D structures, which implies that the graphene always returns to its original position after bending, maintaining its adhesion to the PVA matrix and causing no harm to it.[45] Based on these findings, it is determined that basic PVA films bond to graphene better and that the films remain flexible overall.

3.5. Tensile Strength. The mechanical properties of the composite material show a striking transition when compared between PVA (poly(vinyl alcohol)) in its purest form and PVA with 0.5% graphene reinforcement in the tensile strength tests. Pure PVA exhibits a remarkable tensile strength of 165 MPa (shown in Figure 7) in its original state, demonstrating that it can endure large tensile forces before failing. It is moderately stiff as evidenced by the Young's Modulus of 0.054 MPa. In contrast, a remarkable improvement is seen when just 0.5% graphene is added to the PVA matrix. The composite material is significantly reinforced, as seen by the composite material's explosively high tensile strength of 341 MPa. By making the material more resilient and able to endure significantly higher tensile stresses, graphene plays a crucial role in enhancing the mechanical integrity of the substance as demonstrated by this significant increase. Although the precise Young's modulus value for the PVA-graphene composite is 0.14 MPa, one may anticipate that it will rise as well, indicating the material's increased stiffness as a result of the addition of graphene. Despite being reduced to 129.1%, the elongation at the break still indicates a material with outstanding flexibility, especially in light of the significant increase in tensile strength. Cheng-an et al.[46] show that the composite film's tensile strength grew quickly as the GO content increased. Overall, these findings show graphene's enormous potential as a reinforcing material, providing novel perspectives for the creation of high-performance composite materials with outstanding mechanical properties.[47]

3.6. Water Vapor Transmission Rate (WVTR). PVA is a hydrophilic material with poor moisture barrier properties. To evaluate the WVTR of PVA, a test was conducted using a film test area of 0.0031 cm^2 and a testing time of 10 days, while maintaining the test conditions at 23 °C and 50% RH. The WVTR of pure PVA was found to be 19.3 ± 2.23 g/m^2 day, but the addition of 0.1 vol % graphene reduced it to 6.09 ± 1.65 g/m^2 day. Further addition of 0.2, 0.3, 0.4, and 0.5 vol % graphene resulted in a reduction of 68, 79, 86, 92, and 93%, respectively, with corresponding WVTR values of 4.03 ± 1.29, 2.61 ± 0.93, 1.41 ± 0.68, and 1.22 ± 0.55 g/m^2 day. The WVTR and 1/WVTR values are listed in Table 1. Graphene's

Table 1. Moisture Barrier Property of Polymer and Polymer Nanocomposite Films

film	weight loss (grams)	WVTR (g/m^2 day)	1/WVTR (m^2 day/g)
pristine PVA	0.601	19.38 ± 2.23	0.0516
PVA + 0.1G	0.189	6.09 ± 1.65	0.1642
PVA + 0.2G	0.125	4.03 ± 1.29	0.24814
PVA + 0.3G	0.081	2.61 ± 0.93	0.383142
PVA + 0.4G	0.044	1.41 ± 0.68	0.70922
PVA + 0.5G	0.038	1.22 ± 0.55	0.819672

https://doi.org/10.1021/acsomega.3c02885
ACS Omega 2023, 8, 41054−41063

impermeable nature creates a more tortuous path for gas molecules to pass through the barrier film, leading to the improved barrier quality.[40] Table 1 also shows that increasing the graphene content reduces the weight loss of distilled water through the nanocomposites, indicating a decrease in moisture permeability. Graphene is a single layer of carbon atoms organized in a 2D honeycomb lattice with extraordinary features such as significant mechanical strength, thermal conductivity, and gas and liquid impermeability. When graphene is mixed with PVA, it produces a distributed network within the polymer. Water vapor molecules attempting to diffuse through the PVA composite may encounter a complicated path due to the presence of graphene in the material. The impermeability of graphene works as a barrier, preventing water vapor from passing through the PVA matrix. When compared to pure PVA, which contains the extra barrier supplied by graphene, this behavior reduces the WVTR of the composite. Graphene's sheet-like structure, good aspect ratio, and exfoliation properties also help it to disperse in the PVA matrix and create a hindrance for diffusing molecules by decreasing the free volume of the polymer. SEM also helps examine the film's stability and potential water vapor permeation channels by revealing the distribution of graphene layers and imperfections. Understanding the microstructure of graphene-PVA sheets for low WVTR applications can be guided by SEM investigation, as shown in Figure 5. Controlling the orientation and distribution of graphene sheets within the film can improve its barrier characteristics, lowering the rate of water vapor transmission. The prepared films have excellent moisture barrier properties and can be used in the packaging industry, electronics, fuel cell industry, etc. The improved moisture barrier performance is further illustrated in Figure 8, which shows the inverse of WVTR versus polymer

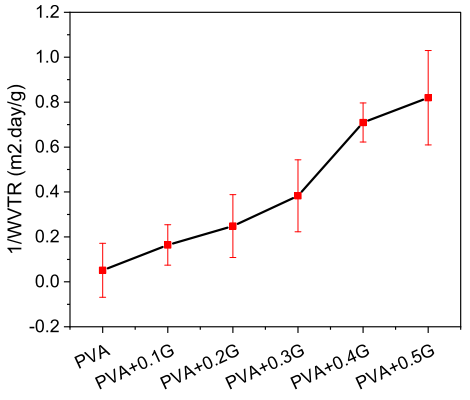

Figure 8. Barrier performance of the polymer nanocomposite film with 0−0.5% variation of graphene in PVA.

nanocomposite films. Introducing nanoparticles or graphene can enhance the blocking effect of the film, and increasing the graphene content from 0.1 to 0.5 vol % decreases 79% of water vapor permeation rate. This indicates a direct relation between graphene content and the inverse of WVTR. The inclusion of nanoparticles has a significant impact on the PVA matrix, as demonstrated by Channa et al.[48] The moisture permeability decreases with increasing glass-flake concentration, which produces an extended route and makes it harder for moisture molecules to disperse. The moisture permeability in the PVA layers with glass-flake concentrations of 5−25 vol % ranged from 6.2 to 1.2 g m^2 day^{-1}.

Bharadwaj proposed a new model for relative permeability that included the aspect ratio of nanoparticles, order parameter S.[49]

$$\frac{P(\text{composite})}{P(\text{polymer})} = \frac{1 - \text{Ø}}{1 + \frac{\alpha}{2}\text{Ø}(\frac{2}{3})(S + \frac{1}{2})} \quad (1)$$

The experimental values of this work were compared to the theoretical permeation model proposed by Bharadwaj. The comparison of the theoretical Bharadwaj permeation model based on aspect ratio; α = 200 and order parameter; S = 0 (suggesting random orientation by supplier) showed similarity with current experimental results as shown in Figure 9. A graph

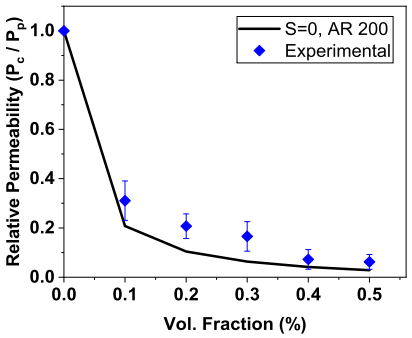

Figure 9. Comparison of experimental relative permeability of PVA films with increasing content of graphene with the Bharadwaj model for an aspect ratio of α = 200 and order parameters of S = 0.

was drawn using eq 1 as a guide. This graph demonstrates that the information provided by the supplier regarding graphene material is accurate and that graphene's interactions with polymers are beneficial to moisture permeability.

Reduction in water vapor permeability through nanocomposite thin film concerning the permeability of pristine PVA is termed the barrier improvement factor (BIF).[50,51] It can be calculated by

$$\text{BIF} = \frac{\text{permeability(polymer)}}{\frac{1 - \text{Ø}}{1 + \frac{\alpha}{2}\text{Ø}(\frac{2}{3})(S + \frac{1}{2})}} \quad (2)$$

where α is the aspect ratio of graphene, S is the order parameter, and Ø is the volume fraction of graphene. Figure 10 shows the increase in BIF with increasing volume fraction of graphene content, confirming the enhancement of barrier performance of graphene and PVA nanocomposites.

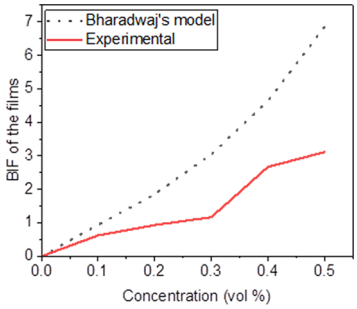

Figure 10. Experimental barrier improvement factor based on graphene content compared with the Bharadwaj model.

https://doi.org/10.1021/acsomega.3c02885
ACS Omega 2023, 8, 41054−41063

3.7. Oxygen Transmission Rate (OTR). Coating and packaging materials need to have oxygen barrier properties to protect objects from internal damage and enhance long-term performance.[52] PVA is known for its exceptional oxygen barrier properties due to its high degree of crystallinity and strong intermolecular force caused by the hydroxyl groups in repeating units.[53] As shown in Figure 11, the addition of

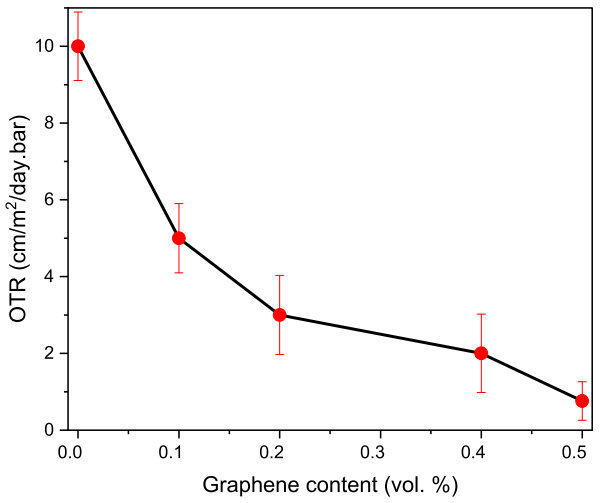

Figure 11. OTR (@0% RH and 25 °C) of PVA films containing different graphene volume concentrations.

graphene to PVA decreased its OTR values (at 0% RH and 25 °C), possibly due to the graphene nanocomposite and PVA matrix being designed with an incredibly tortuous path to prevent oxygen molecules from penetrating through it. The development of highly oriented 2D filler-based coatings is responsible for the superior oxygen barrier property. Gaume et al.[54] also examined the permeability of nanocomposites and demonstrated that 5 wt % of MMt-Na+ enhanced helium permeability (by 70%), as well as oxygen and water permeability. The OTRs of PVA/G composite films are significantly lower compared to pure PVA films, indicating improved barrier properties of graphene by the polymerization of PVA. These findings imply that a PVA matrix with uniformly dispersed graphene can be produced due to the enhanced compatibility between PVA/G and the PVA matrix. Furthermore, the increased quantity of strong hydrogen bonds results in a longer diffusion pathway and more contact between PVA-G and the PVA matrix, which decreases oxygen transmission. Although the optical transmittance drops when the PVA-G concentration rises (Figure 1), the barrier characteristics are still suitable for gas barrier films due to the improved compatibility of PVA-G and the PVA matrix.

3.8. Thermal Stability. The thermogravimetric analysis (TGA) and corresponding differential thermogravimetric analysis (DTG) in an inert atmosphere were used to evaluate the nanocomposite materials' thermal stability.[55] As shown in Figure 12, the weight loss of the PVA film steadily increases with temperature, with inflection points at 85.7, 210.9, and 390.5 °C. According to ref 56, this weight loss can be attributed to the dehydration of the PVA chain and the formation of a polyacetylene-like structure at temperatures between 200 and 300 °C, the evaporation of adsorbed water in the PVA chain at temperatures between 60 and 150 °C, and the main chain disintegration of PVA at temperatures between

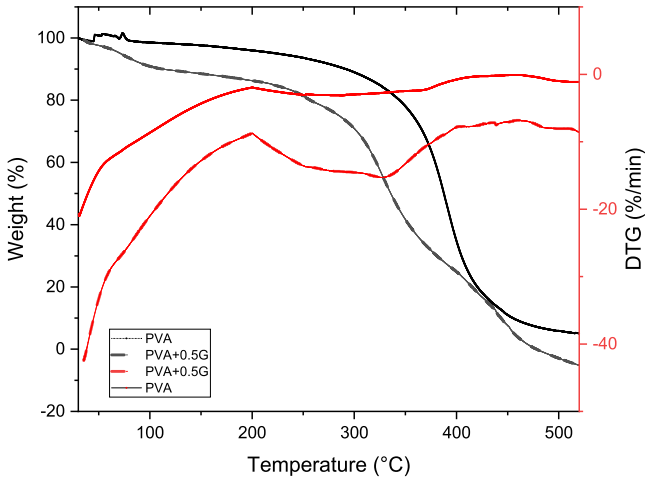

Figure 12. Thermogravimetric analysis (TGA) of the simple PVA film is represented by a black dotted line and the simple black line represents the PVA + 0.5G film. Differential thermogravimetric analysis (DTG) of the simple PVA film is represented by a red simple line and a red dotted red line representing the PVA + 0.5G film.

380 and 470 °C (as shown in Table 2). The weight loss of the PVA-G film with 5 vol % exhibits a trend similar to that of the

Table 2. Film Thermal Gravimetric Analysis Data

sample	T_i (decomposition temperature)	T_f (final temperature)
PVA + 0.5G	120.7 °C	430.5 °C
PVA	280.81 °C	400.3 °C

PVA film with increasing temperature, as shown in Figure 12. This suggests that adding nanomaterial can increase the thermal stability of the polymer matrix. At this stage, the PVA nanocomposite film and the pure PVA film showed similar levels of stability. The stages of deterioration observed in the PVA film also coincided with those of the PVA film containing graphene. At the end of the thermal deterioration process, the weight loss concentration of the PVA film with graphene was 7.65%.

4. CONCLUSIONS

Graphene-based nanocomposites are a novel type of material with potential applications in numerous fields. In this study, we present a general procedure for synthesizing poly(vinyl alcohol) (PVA)/graphene (G) nanocomposites using a simple solution-mixing approach. Both materials are cost-effective, widely available, and durable. To evaluate the properties of the produced materials, we conducted tests such as thermogravimetric, water vapor transmission rate, oxygen transmission rate, tensile strength, SEM, UV−vis spectroscopy, and FTIR spectroscopy. By using ultra sonication, we achieved an even distribution of graphene nanoparticles throughout the PVA matrix as confirmed by a SEM image, effectively preventing nanoparticle restacking. The strong interfacial connection between PVA and graphene, which was primarily due to hydrogen bonding and enhancement of the PVA crystallinity, improved the mechanical and thermal stability of the nanocomposites. Our tests showed that the addition of just 0.5 vol % graphene concentrations to the PVA film reduced the water vapor transmission rate from 19 to 1.22 g m^{-2} day^{-1} and the oxygen transmission rate from 10 to 0.5 cm m^{-2} day^{-1}

https://doi.org/10.1021/acsomega.3c02885
ACS Omega 2023, 8, 41054−41063

bar^{-1}. Furthermore, graphene increased the thermal stability and tensile strength of the polymer nanocomposite film. We were able to produce the films at a lab scale for less than 0.6 USD/m^2. These findings suggest that PVA/G nanocomposites have the potential for use in various coating and packaging films to protect against moisture and corrosion.

AUTHOR INFORMATION

Corresponding Author

Iftikhar Ahmed Channa − *Thin Film Lab as Part of Materials and Surface Engineering Group, Department of Metallurgical Engineering, NED University of Engineering and Technology, Karachi 75270, Pakistan*; Email: iftikharc@neduet.edu.pk

Authors

Jaweria Ashfaq − *Thin Film Lab as Part of Materials and Surface Engineering Group, Department of Metallurgical Engineering, NED University of Engineering and Technology, Karachi 75270, Pakistan*

Abdul Ghaffar Memon − *State Key Joint Laboratory of ESPC, School of Environment, Tsinghua University, Beijing 100084, China; Department of Environmental Engineering, NED University of Engineering and Technology, Karachi 75270, Pakistan*

Irfan Ali Chandio − *Department of Telecommunication Engineering, Dawood University of Engineering and Technology, Karachi 74800, Pakistan*

Ali Dad Chandio − *Thin Film Lab as Part of Materials and Surface Engineering Group, Department of Metallurgical Engineering, NED University of Engineering and Technology, Karachi 75270, Pakistan*; orcid.org/0000-0003-4115-2070

Muhammad Ali Shar − *Departments of Mechanical & Energy Systems Engineering, Faculty of Engineering and Informatics, University of Bradford, Bradford BD7 1DP, U.K.*

Mohamad S. Alsalhi − *Departments of Physics and Astronomy, College of Science, King Saud University, Riyadh 11451, Saudi Arabia*

Sandhanasamy Devanesan − *Departments of Physics and Astronomy, College of Science, King Saud University, Riyadh 11451, Saudi Arabia*

Complete contact information is available at: https://pubs.acs.org/10.1021/acsomega.3c02885

Author Contributions

Conceptualization, A.D.C. and I.A.C.; methodology, A.G.M, J.A., and I.A.C. (Irfan Ali Chandio); writing, I.A.C. and J.A.; validation, I.A.C., M.S.A., S.D., and A.D.C.; investigation, J.A., I.A.C., A.G.M., M.A.S., and I.A.C. (Irfan Ali Chandio); supervision, A.D.C.; funding acquisition, M.A.S., S.D., M.S.A., I.A.C., and A.D.C. All authors have read and agreed to the published version of the manuscript.

Funding

The authors express their sincere appreciation to the Researchers Supporting Project number (RSP2023R68) at King Saud University, Riyadh, Saudi Arabia, and the APC was funded by RSP.

Notes

The authors declare no competing financial interest.

ACKNOWLEDGMENTS

The authors express their sincere appreciation to the Researchers Supporting Project number (RSP2023R68) at King Saud University, Riyadh, Saudi Arabia.

REFERENCES

(1) Channa, I. A. Development of Solution Processed Thin Film Barriers for Encapsulating Thin Film Electronics Entwicklung von Lösungsprozessierten Dünnschichtbarrieren Für Die Verpackung von Dünnschichtelektronik, 2019.

(2) Giwa, A. S.; Sheng, M.; Zhang, X.; Wu, Y.; Bo, H.; Memon, A. G.; Bai, S.; Ali, N.; Ndungutse, J. M.; Kaijun, W. Approaches for Treating Domestic Wastewater with Food Waste and Recovery of Potential Resources. *Environ. Pollut. Bioavail.* **2022**, *34*, 501−517.

(3) Azmin, S. N. H. M.; Hayat, N. A.; Binti, M.; Nor, M. S. M. Development and Characterization of Food Packaging Bioplastic Film from Cocoa Pod Husk Cellulose Incorporated with Sugarcane Bagasse Fibre. *J. Bioresour. Bioprod.* **2020**, *5*, 248−255.

(4) Dilucia, F.; Lacivita, V.; Conte, A.; Nobile Del, M. A. Sustainable Use of Fruit and Vegetable By-Products to Enhance Food Packaging Performance. *Foods* **2020**, *9*, 857.

(5) Gupta, V.; Biswas, D.; Roy, S. A Comprehensive Review of Biodegradable Polymer-Based Films and Coatings and Their Food Packaging Applications. *Materials* **2022**, *15*, 5899.

(6) Ramos, M.; Valdés, A.; Beltrán, A.; Garrigós, M. Gelatin-Based Films and Coatings for Food Packaging Applications. *Coatings* **2016**, *6*, 41.

(7) Channa, I. A.; Ashfaq, J.; Siddiqui, M. A.; Chandio, A. D.; Shar, M. A.; Alhazaa, A. Multi-Shaded Edible Films Based on Gelatin and Starch for the Packaging Applications, 2022.

(8) Maitlo, G.; Abbasi, S. A.; Korai, R. M.; Memon, A. G. Perspective of Bioenergy in Pakistan for Sustainable Eco-Friendly Energy Substitute: A Review. *Mehran Univ. Res. J. Eng. Technol.* **2021**, *40*, 591−605.

(9) Bala, A.; Arfelis, S.; Oliver-Ortega, H.; Méndez, J. A. Life Cycle Assessment of PE and PP Multi Film Compared with PLA and PLA Reinforced with Nanoclays Film. *J. Clean. Prod.* **2022**, *380*, No. 134891.

(10) Martin, M.; Prasad, N.; Sivalingam, M. M.; Sastikumar, D.; Karthikeyan, B. Optical, Phonon Properties of ZnO−PVA, ZnO−GO−PVA Nanocomposite Free Standing Polymer Films for UV Sensing. *J. Mater. Sci.: Mater. Electron.* **2018**, *29*, 365−373.

(11) Yang, Z.; Peng, H.; Wang, W.; Liu, T. Crystallization Behavior of Poly(ε-Caprolactone)/Layered Double Hydroxide Nanocomposites. *J. Appl. Polym. Sci.* **2010**, *116*, 2658−2667.

(12) Drusilla Wendy, Y. B.; Nor Fauziah, M. Z.; Siti Baidurah, Y.; Tong, W. Y.; Lee, C. K. Production and Characterization of Polyhydroxybutyrate (PHB) BY Burkholderia Cepacia BPT1213 Using Waste Glycerol as Carbon Source. *Biocatal. Agric. Biotechnol.* **2022**, *41*, No. 102310.

(13) Regubalan, B.; Manibalan, S.; Pandit, P. 9 - Polyglycolic Acid-Based Bionanocomposites for Food Packaging Applications. In *Woodhead Publishing Series in Composites Science and Engineering*; Ahmed, S.B.T.-B. for F.P.A., Ed.; Woodhead Publishing, 2022; pp 153−164. ISBN 978-0-323-88528-7.

(14) Song, J. H.; Murphy, R. J.; Narayan, R.; Davies, G. B. H. Biodegradable and Compostable Alternatives to Conventional Plastics. *Philos. Trans. R. Soc. B: Biol. Sci.* **2009**, *364*, 2127−2139.

(15) Oyeoka, H. C.; Ewulonu, C. M.; Nwuzor, I. C.; Obele, C. M.; Nwabanne, J. T. Packaging and Degradability Properties of Polyvinyl Alcohol/Gelatin Nanocomposite Films Filled Water Hyacinth Cellulose Nanocrystals. *J. Bioresour. Bioprod.* **2021**, *6*, 168−185.

(16) Wu, Z.; Wu, J.; Peng, T.; Li, Y.; Lin, D.; Xing, B.; Li, C.; Yang, Y.; Yang, L.; Zhang, L.; et al. Preparation and Application of Starch/Polyvinyl Alcohol/Citric Acid Ternary Blend Antimicrobial Functional Food Packaging Films. *Polymers* **2017**, *9*, 1−19.

(17) Abdullah, Z.; Dong, Y.; Davies, I.; Barbhuiya, S. PVA, PVA Blends and Their Nanocomposites for Biodegradable Packaging Application. *Polym. Plast. Technol. Eng.* **2017**, *56*, 1307−1344.
(18) Chandio, A. D.; Channa, I. A.; Rizwan, M.; Akram, S.; Javed, M. S.; Siyal, S. H.; Saleem, M.; Makhdoom, M. A.; Ashfaq, T.; Khan, S.; et al. Polyvinyl Alcohol and Nano-Clay Based Solution Processed Packaging Coatings. *Coatings* **2021**, *11*, No. 080942.
(19) Laxmiprasanna, N.; Sandeep Reddy, P.; Shiva Kumar, G.; Balakrishna Reddy, M.; Ganta, K. K.; Jeedi, V. R.; Praveen, B. V. S. A Review on Nano Composite Polymer Electrolytes for High-Performance Batteries. *Mater. Today Proc.* **2023**, *72*, 286.
(20) Pendergast, M. M.; Hoek, E. M. V. A Review of Water Treatment Membrane Nanotechnologies. *Energy Environ. Sci.* **2011**, *4*, 1946−1971.
(21) Channa, I. A.; Distler, A.; Brabec, C. J.; Egelhaaf, H.-J. 9 - Solution-Coated Barriers for Organic Electronics. In *Woodhead Publishing Series in Electronic and Optical Materials*; Cosseddu, P., Caironi, M.B.T.-O.F.E., Eds.; Woodhead Publishing, 2021; pp 249−303. ISBN 978−0-12−818890−3.
(22) Karki, S.; Gohain, M. B.; Yadav, D.; Ingole, P. G. Nanocomposite and Bio-Nanocomposite Polymeric Materials/Membranes Development in Energy and Medical Sector: A Review. *Int. J. Biol. Macromol.* **2021**, *193*, 2121−2139.
(23) Kim, J.; Kang, T.; Kim, H.; Shin, H. J.; Oh, S.-G. Preparation of PVA/PAA Nanofibers Containing Thiol-Modified Silica Particles by Electrospinning as an Eco-Friendly Cu (II) Adsorbent. *J. Ind. Eng. Chem.* **2019**, *77*, 273−279.
(24) Chandio, A. D.; Pato, A. H.; Channa, I. A.; Gilani, S. J.; Shah, A. A.; Ashfaq, J.; Buledi, J. A.; Chandio, I. A.; Jumah, M. N. Bin Exploring the Heterocatalytic Proficiencies of ZnO Nanostructures in the Simultaneous Photo-Degradation of Chlorophenols. *Sustainability* **2022**, *14*, 14562.
(25) Sajid, M. Nanomaterials: Types, Properties, Synthesis, Emerging Materials, and Toxicity Concerns. *Curr. Opin. Environ. Sci. Heal.* **2022**, *25*, No. 100319.
(26) Mansourpanah, Y. MXenes and Other 2D Nanosheets for Modification of Polyamide Thin Film Nanocomposite Membranes for Desalination. *Sep. Purif. Technol.* **2022**, *289*, No. 120777.
(27) Liu, G.; Jin, W.; Xu, N. Graphene-Based Membranes. *Chem. Soc. Rev.* **2015**, *44*, 5016−5030.
(28) Alagumalai, A.; Yang, L.; Ding, Y.; Marshall, J. S.; Mesgarpour, M.; Wongwises, S.; Rashidi, M. M.; Taylor, R. A.; Mahian, O.; Sheremet, M.; et al. Nano-Engineered Pathways for Advanced Thermal Energy Storage Systems. *Cell Rep. Phys. Sci.* **2022**, *3*, No. 101007.
(29) Abro, S. H.; Chandio, A.; Alaboodi, A. S.; Channa, I.A. Design Development and Characterization of Graphene Sand Nano-Composite for Water Filtration. *Pak. J. Sci. Ind. Res. Ser. A Phys. Sci.* **2020**, *63*, 118−122.
(30) Singh, E.; Meyyappan, M.; Nalwa, H. S. Flexible Graphene-Based Wearable Gas and Chemical Sensors. *ACS Appl. Mater. Interfaces* **2017**, *9*, 34544−34586.
(31) Tambe, P.; Sharma, A.; Kulkarni, H.; Panda, B. Solvent Assisted Dispersion of Graphene and Its PVA Nanocomposites Coating: Processing and Characterization. *Mater. Today Proc.* **2022**, *56*, 1383−1390.
(32) Krishnan, S.; Singh, E.; Singh, P.; Meyyappan, M.; Nalwa, H. S. A Review on Graphene-Based Nanocomposites for Electrochemical and Fluorescent Biosensors. *RSC Adv.* **2019**, *9*, No. 09577A.
(33) Tavares, M. I. B.; da Silva, E. O.; da Silva, P. R. C.; de Menezes, L.R. Polymer Nanocomposites; Seehra, M. S., Ed.; IntechOpen: Rijeka, 2017; p. Ch. 7. ISBN 978-953-51-3372-8.
(34) Hamadneh, N.; Khan, W.; Khan, W. Polymer Nanocomposites − Synthesis Techniques, Classification and Properties, 2016. ISBN 978-1-910086-19-3.
(35) Vollenberg, P. H. T.; Heikens, D. Particle Size Dependence of the Young's Modulus of Filled Polymers: 1. Preliminary Experiments. *Polymer* **1989**, *30*, 1656−1662.
(36) Channa, I. A.; Distler, A.; Scharfe, B.; Feroze, S.; Forberich, K.; Lipovšek, B.; Brabec, C. J.; Egelhaaf, H. J. Solution Processed Oxygen and Moisture Barrier Based on Glass Flakes for Encapsulation of Organic (Opto-) Electronic Devices. *Flex. Print. Electron.* **2021**, *6*, 25006.
(37) Yahia, I. S.; Mohammed, M. I. Facile Synthesis of Graphene Oxide/PVA Nanocomposites for Laser Optical Limiting: Band Gap Analysis and Dielectric Constants. *J. Mater. Sci.: Mater. Electron.* **2018**, *29*, 8555−8563.
(38) Morimune, S.; Nishino, T.; Goto, T. Poly(Vinyl Alcohol)/Graphene Oxide Nanocomposites Prepared by a Simple Eco-Process. *Polym. J.* **2012**, *44*, 1056−1063.
(39) Ahmad, J.; Memon, A. G.; Shaikh, A. A.; Ismail, T.; Giwa, A. S.; Mahmood, A. Insight into Single-Element Nobel Metal Anisotropic Silver Nanoparticle Shape-Dependent Selective ROS Generation and Quantification. *RSC Adv.* **2021**, *11*, 8314−8322.
(40) Sudsandee, S.; Chien-Chieh; Liu, Y.-L.; Worakhunpiset, S.; Loahaprapanon, Sawanya; Wei-Song Hung, B. D.; Kueir-Rarn Lee, D. J.-Y.L. Improving Barrier Performance of Transparent Polymeric Film Using Silk Nanofibril Combine Graphene Oxide. *J. Taiwan Inst. Chem. Eng.* **2018**, *409−410*, 156−163.
(41) Alsaad, A. M.; Ahmad, A. A.; Al Dairy, A. R.; Al-anbar, A. S.; Al-Bataineh, Q. M. Spectroscopic Characterization of Optical and Thermal Properties of (PMMA-PVA) Hybrid Thin Films Doped with SiO2 Nanoparticles. *Results Phys.* **2020**, *19*, No. 103463.
(42) You, S.; Luzan, S. M.; Szabó, T.; Talyzin, A. V. Effect of Synthesis Method on Solvation and Exfoliation of Graphite Oxide. *Carbon N. Y.* **2013**, *52*, 171−180.
(43) Mutyala, S.; Mathiyarasu, J. Preparation of Graphene nanoflakes and Its Application for Detection of Hydrazine. *Sens. Actuators, B* **2015**, *210*, 692−699.
(44) Chandio, A. D.; Shaikh, A. A.; Channa, I. A.; Bacha, M. S.; Bhatti, J.; Khan, M. Y.; Bhutto, S. Synthesis of Graphene Oxide (GO) by Modified Hummer's Method with Improved Oxidation through Ozone Treatment. *J. Chem. Soc. Pakistan* **2023**, No. 1−7, 45.
(45) Zhang, P.; Ling, Y.; Wang, J.; Shi, Y. Bending Resistance of PVA Fiber Reinforced Cementitious Composites Containing Nano-SiO 2, 2019; pp 690−698.
(46) Cheng-An, T.; Hao, Z.; Fang, W.; Hui, Z.; Xiaorong, Z.; Jianfang, W. Mechanical Properties of Graphene Oxide/Polyvinyl Alcohol Composite Film. *Polym. Polym. Compos.* **2017**, *25*, 11−16.
(47) Sarwar, M. S.; Niazi, M. B. K.; Jahan, Z.; Ahmad, T.; Hussain, A. Preparation and Characterization of PVA/Nanocellulose/Ag Nanocomposite Films for Antimicrobial Food Packaging. *Carbohydr. Polym.* **2018**, *184*, 453−464.
(48) Channa, I.; Distler, A.; Scharfe, B.; Feroze, S.; Forberich, K.; Lipovšek, B.; Brabec, C.; Egelhaaf, H.-J. Solution Processed Oxygen and Moisture Barrier Based on Glass Flakes for Encapsulation of Organic (Opto-) Electronic Devices. *Flex. Print. Electron.* **2021**, *6*, No. ac0716.
(49) Bharadwaj, R. K. Modeling the Barrier Properties of Polymer-Layered Silicate Nanocomposites. *Macromolecules* **2001**, *34*, 9189−9192.
(50) Liu, J.; Zhang, L.; Liu, C.; Zheng, X.; Tang, K. Tuning Structure and Properties of Gelatin Edible Films through Pullulan Dialdehyde Crosslinking. *LWT* **2021**, *138*, No. 110607.
(51) Channa, I. A.; Chandio, A. D.; Rizwan, M.; Shah, A. A.; Bhatti, J.; Shah, A. K.; Hussain, F.; Shar, M. A.; AlHazaa, A. Solution Processed PVB/Mica Flake Coatings for the Encapsulation of Organic Solar Cells. *Materials* **2021**, *14*, 2496.
(52) Lee, M. E.; Jin, H. J. Nanocomposite Films of Poly(Vinyl Alcohol)-Grafted Graphene Oxide/Poly(Vinyl Alcohol) for Gas Barrier Film Applications. *J. Nanosci. Nanotechnol.* **2015**, *15*, 8348−8352.
(53) Wang, X.; Li, X.; Cui, L.; Liu, Y.; Fan, S. Improvement of Gas Barrier Properties for Biodegradable Poly(Butylene Adipate-Co-Terephthalate) Nanocomposites with MXene Nanosheets via Biaxial Stretching. *Polymers* **2022**, *14*, 480.

https://doi.org/10.1021/acsomega.3c02885
ACS Omega 2023, 8, 41054−41063

(54) Gaume, J.; Taviot-Gueho, C.; Cros, S.; Rivaton, A.; Thérias, S.; Gardette, J.-L. Optimization of PVA Clay Nanocomposite for Ultra-Barrier Multilayer Encapsulation of Organic Solar Cells. *Sol. Energy Mater. Sol. Cells* **2012**, *99*, 240−249.
(55) Bratovcic, A. Physical − Chemical, Mechanical and Antimicrobial Properties of Bio-Nanocomposite Films and Edible Coatings. *Int. J. Res. Appl. Sci. Biotechnol.* **2021**, *8*, 151−161.
(56) Wu, Z.; Huang, Y.; Xiao, L.; Lin, D.; Yang, Y.; Wang, H.; Yang, Y.; Wu, D.; Chen, H.; Zhang, Q.; et al. Physical Properties and Structural Characterization of Starch/Polyvinyl Alcohol/Graphene Oxide Composite Films. *Int. J. Biol. Macromol.* **2019**, *123*, 569−575.

https://doi.org/10.1021/acsomega.3c02885
ACS Omega 2023, 8, 41054−41063